ELSEVIER

www.elsevier.nl/locate/jorganchem

Journal of Organometallic Chemistry 597 (2000) 20–28

Journal of Organometallic Chemistry

Molecular structure and properties of the rhodium(II) complexes with chemilabile ether–phosphine ligands P(2-$MeOC_6H_4)_3$ and P(2,6-$(MeO)_2C_6H_3)_3$

Florian P. Pruchnik [a,*], Radosław Starosta [a], Maria W. Kowalska [a], Ewa Gałdecka [b], Zdzisław Gałdecki [c], Andrzej Kowalski [d]

[a] *Faculty of Chemistry, University of Wrocław, 14 F. Joliot-Curie Street, PL-50383 Wrocław, Poland*
[b] *Institute of Low Temperature and Structure Research, Polish Academy of Sciences, Okólna 2, PL-50950 Wrocław, Poland*
[c] *Institute of General and Ecological Chemistry, Technical University of Łódź, Żwirki 36, PL-90924 Łódź, Poland*
[d] *Kuma Diffraction Ltd., ul. Akacjowa 15b, PL-53122 Wrocław, Poland*

Received 16 June 1999; received in revised form 3 September 1999

Abstract

Reactions of dirhodium tetraacetate [$Rh_2(O_2CCH_3)_4$] with tris(2-methoxyphenyl)phosphine (OMP) yield the oxygen-metallated complexes [$Rh_2(\mu$-$OAc)_3\{\mu$-(2-$OC_6H_4)P$(2-$MeOC_6H_4)_2\}$(HOAc)] (**1**·HOAc) and [$Rh_2(\mu$-$OAc)_3\{\mu$-(2-$OC_6H_4)P$(2-$MeOC_6H_4)_2\}$-(NCMe)] (**1**·NCMe). In the case of tris(2,6-dimethoxyphenyl)phosphine (DOMP) analogous compound [$Rh_2(\mu$-$OAc)_3\{\mu$-(2-O-(6-MeO)$C_6H_3)P$(2,6-$(MeO)_2C_6H_3)_2\}$(HOAc)] (**2**·HOAc) was obtained. In both ligands the CH_3^+ cation of one of the methoxy substituents is split off and the phosphine replaces one of the acetato bridges to form the bridge with Rh_2^{4+} core closing the six-member ring via P and O atoms. The compounds have been characterized using UV–vis, IR, ^{1}H-, ^{13}C{^{1}H}- and ^{31}P{^{1}H}-NMR spectroscopies. The crystal structure of compound **1**·NCMe has been determined. The Rh(1)–Rh(2) distance is distinctly longer than that in [$Rh_2(OAc)_4(H_2O)_2$] (**3**·2H_2O). Axial sites of dirhodium core are occupied by a molecule of acetonitrile and a methoxy group of one of the nonmetallated phenyl rings. Detailed NMR studies reveal dynamic properties of complex **1** involving exchange between axial methoxy substituents and tilting of the metallated ring. The complexes **1** and **2** react with carbon monoxide giving complexes with a CO ligand coordinated in axial coordination sites.

Keywords: Carbon monoxide; Dirhodium complexes; Ether–phosphines

1. Introduction

Creating weak and fluctional bonds of oxygen to metal centers has been used to advantage in homogeneous catalysis. Although ether–phosphines are the subject of growing interest because of their ability to coordinate via phosphorus and oxygen atoms, their reactions with dirhodium(II) tetracarboxylates are not widely investigated. Only few examples of such complexes are known [1–5].

Reactions of dirhodium(II) tetracarboxylates and their derivatives with carbon monoxide were not thoroughly investigated. Only few examples of such complexes, containing coordinated CO, are known. The crystal structure of [$Rh_2(OAc)_4(CO)_2$] (**3**·2CO) [6] and reactivity of **3** towards CO at high pressures [7] were described. There are also published chemical studies on tertabutyrato-, tetrakis (perfluorobutyrato)- and tetrakis (2-anilinopyridinato) dirhodium(II) adducts with CO [8–10].

In this work we present the crystal structure of [$Rh_2(\mu$-$OAc)_3\{\mu$-(2-$OC_6H_4)P$(2-$MeOC_6H_4)_2\}$(NCMe)] (**1**·NCMe) and spectroscopic studies of [$Rh_2(\mu$-$OAc)_3$-$\{\mu$-(2-$OC_6H_4)P$(2-$MeOC_6H_4)_2\}$(HOAc)] (**1**·HOAc) and [$Rh_2(\mu$-$OAc)_3\{\mu$-(2-O-(6-MeO)$C_6H_3)P$(2,6-$(MeO)_2C_6$-$H_3)_2\}$(HOAc)] (**2**·HOAc) as well as reactions of **1**, **2** and **3** with CO under atmospheric pressure.

* Corresponding author. Fax: +48-71-3204232.
E-mail address: pruchnik@wchuwr.chem.uni.wroc.pl (F.P. Pruchnik)

0022-328X/00/$ - see front matter
PII: S0022-328X(99)00529-X

2. Results and discussion

Compounds **1** and **2** have been characterized by a combination of MS, IR, UV–vis, ^{1}H- and ^{31}P-NMR spectroscopies and elemental analysis. The molecular structure of complex **1**·NCMe has been determined by X-ray diffraction. $^{31}P\{^1H\}$- and ^{1}H-NMR spectra and the assignments (supported by $^1H\{^{31}P\}$ spectra) are given in Table 1.

2.1. Reactions of formation of adducts of $Rh_2(OAc)_4$ with OMP

For most adducts $[(Rh_2(OAc)_4PR_3]$ and $[(Rh_2(OAc)_4(PR_3)_2]$ with alkyl and aryl phosphines without oxygen atoms in the *ortho* position to phosphorus, atom coordination chemical shifts $\Delta\delta = \delta(P_{adduct}) - \delta(P_{free\ phosphine})$ are about -30 and -10 ppm, respectively [1,11–18]. However, in mixtures of $[(Rh_2(OAc)_4]$ (**3**) with tris(2-methoxyphenyl)phosphine (OMP) at 1:1 and 1:2 molar ratios in the $^{31}P\{^1H\}$-NMR spectrum, only significant broadening of the signal without changing the chemical shifts was observed. For adducts of **3** with similar phosphine P(2-$MeOC_6H_4)(C_6H_5)_2$ the values of coordination chemical shifts $\Delta\delta$ are -23 ppm for the monoadduct and -4 ppm for the bisadduct, which are in a sense halfway between the adducts of **3** with nonfunctionalized aryl phosphines and adducts with OMP. At lower temperatures (273–213 K) $^{31}P\{^1H\}$-NMR spectra of adducts with OMP show two signals: a singlet of chemical shift of free OMP and a doublet of doublets (^1J(Rh–P) ≈ 96.0, ^2J(Rh–P) ≈ 30 Hz) moved to upper fields. The difference in chemical shifts between this pair of signals changes from 4 to 2 ppm with a decrease in temperature. Analysis of proton spectra shows that only one adduct is formed over this temperature range. Analysis of relative intensities of signals of –OMe groups at 243 K indicates the following amounts of compounds: in the 1:1 mixture 35% of free OMP and 65% of adduct, in the 1:2 mixture 58% of free OMP and 42% of adduct. In the aromatic range of that spectrum signals of the H^3, H^4 and H^5 in the adduct change their positions only slightly (about ± 0.1 ppm); however the signal of H^6 is moved to a lower field by 1 ppm. Most probably, in these reactions, only the monoadduct (**3**·OMP) is formed due to steric hindrances. Analysis of the spectrum mentioned above also allowed us to assign all signals of the free ligand (Table 1), in which $^4J(H^3–P)$ and $^3J(H^6–P)$ are unexpectedly almost the same, 4.8 and 4.4 Hz, respectively.

2.2. Molecular structure and dynamic properties of *1·HOAc*

The $^{31}P\{^1H\}$-NMR spectrum of complex **1**·HOAc reveals a doublet centered at 33.3 ppm (^1J(P–Rh) = 157 Hz) which does not change within a wide range of temperatures (313–213 K). The difference between phosphorus chemical shifts in **1**·HOAc and in the free

Table 1
^{1}H- and $^{31}P\{^1H\}$-NMR spectra (in $CDCl_3$, at r.t.)

Complex	Spectrum	Chemical shifts (ppm) [bold] and coupling constants (Hz)
OPM	$^{31}P\{^1H\}$	**−39.5** (s)
	^{1}H	**3.72** (s, 9H^{OMe}), **7.29** (td, 3H^4) $^3J(H^4–H^5) \approx {}^3J(H^4–H^3) = 7.48$ $^3J(H^4–H^6) = 1.72$, **6.86** (dd, 3H^3) $^4J(H^3–P) = 4.84$, **6.81** (t, 3H^5) $^3J(H^5–H^4) \approx {}^3J(H^5–H^6)$, **6.67** (ddd, 3H^6) $^3J(H^6–P) = 4.35$
DOMP	$^{31}P\{^1H\}$	**−66.9** (s)
	^{1}H	**3.44** (s, H^{OMe}), **7.09** (t, 3H^4) $^3J(H^4–H^3,H^5) = 8.07$, **6.40** (dd, 3H^3,3H^5) $^3J(H^3,H^5–H^4) = 7.77$ $^4J(H^3,H^5–P) = 3.42$, **6.67** (ddd, 3H^3) $^4J(H^3–P) = 4.35$
1·HOAc	$^{31}P\{^1H\}$	**33.4** (d) ^1J(P–Rh) = 157
	^{1}H	**1.18** (s, 6H$^{-OAc\text{-}cis}$), **2.30** (s, 3H$^{-OAc\text{-}trans}$), **2.16** (s, 6H$^{-HOAc\text{-}axial}$), **3.99** (s *, 6H^{OMe}), **7.4–6.6** (aromatic protons)
2·HOAc	$^{31}P\{^1H\}$	**13.6** (d) ^1J(P–Rh) = 151
	^{1}H	**1.24** (s, 3H^{-OAc}), **1.45** (s, 3H^{-OAc}), **1.99** (s, 3H^{-OAc}), **2.15** (s, 3H^{-OAc}), **3.19** (s, 3H^{-OMe}), **3.36** (s, 3H^{-OMe}), **3.41** (s, 3H^{-OMe}), **3.44** (s, 3H^{-OMe}), **4.68** (s, 3H^{-OMe}), **6.06** (dd) ^3J(H–H) = 7.96, ^4J(H–P) = 5.24, **6.16** (dd) ^3J(H–H) = 7.98, ^4J(H–P) = 4.68, **6.34** (dd) ^3J(H–H) = 7.98, ^4J(H–P) = 3.57, **6.48** (dd) ^3J(H–H) = 8.25, ^4J(H–P) = 2.19, **6.53** (dd) ^3J(H–H) = 8.52, ^4J(H–P) = 5.76, **6.92** (dd) ^3J(H–H) = 8.50, ^4J(H–P) = 4.66, **6.97** (t) $^3J(H–H) \approx {}^4J$(H–P) = 8.25, **7.11** (t) $^3J(H–H) \approx {}^4J$(H–P) = 8.25, **7.38** (t) $^3J(H–H) \approx {}^4J$(H–P) = 8.24
2·CO	$^{31}P\{^1H\}$	**8.85** (d *) ^1J(P–Rh) = 161
	^{1}H	**1.23** (s, 3H^{-OAc}), **1.48** (s, 3H^{-OAc}), **2.14** (s, 3H^{-OAc}), **3.20** (s, 3H^{-OMe}), **3.34** (s, 3H^{-OMe}), **3.41** (s, 6H^{-OMe}), **4.60** (s, 3H^{-OMe}), **6.12** (dd) ^3J(H–H) = 8.24, ^4J(H–P) = 4.60, **6.18** (dd) ^3J(H–H) = 8.02, ^4J(H–P) = 4.82, **6.30** (dd) ^3J(H–H) = 8.23, ^4J(H–P) = 3.40, **6.45** (d *) ^3J(H–H) = 8.43, **6.58** (dd) ^3J(H–H) = 7.62, ^4J(H–P) = 5.22, **6.86** (dd) ^3J(H–H) = 8.43, ^4J(H–P) = 4.80, **7.01** (t) $^3J(H–H) \approx {}^4J$(H–P) = 8.02, **7.08** (t) $^3J(H–H) \approx {}^4J$(H–P) = 8.22, **7.36** (t) $^3J(H–H) \approx {}^4J$(H–P) = 8.24

* Significantly broadened signal.

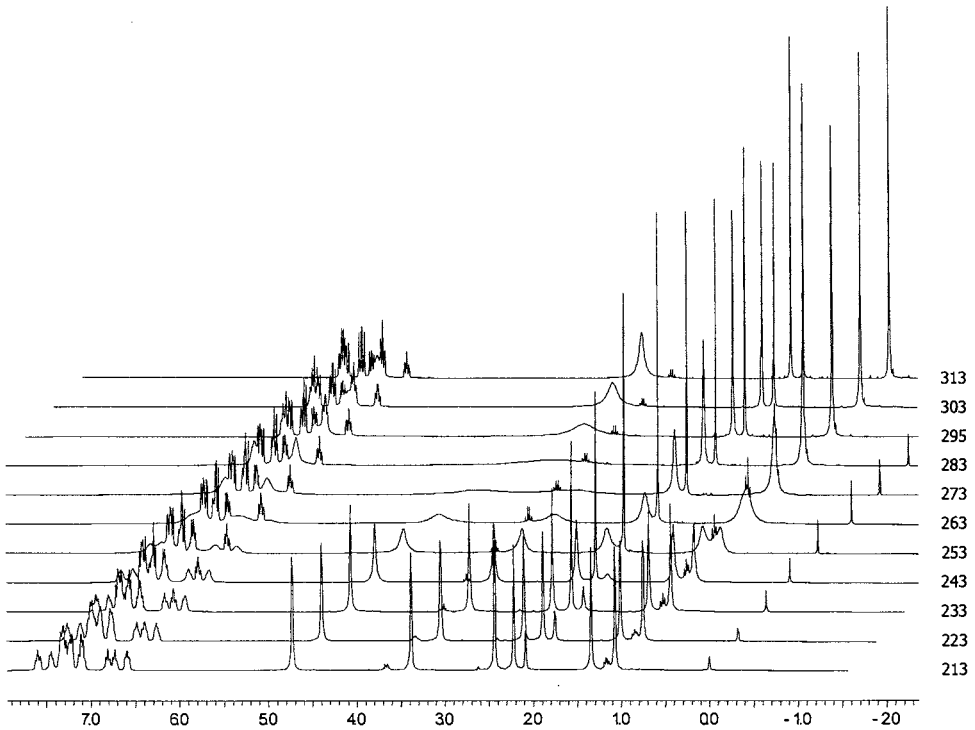

Fig. 1. View of ^{1}H-NMR spectra of **1**·HOAc in $CDCl_3$ at different temperatures.

ligand ($\Delta\delta \approx 73$ ppm) is much larger than in most complexes with equatorial or C-metallated phosphine and comparable to the analogous difference (~ 80 ppm) in the similar complex $[Rh_2(OAc)_3\{(2\text{-}OC_6H_2(OMe)_2)P(C_6H_2(OMe)_3)_2\}(MeOH)]$ described by Chen and Dunbar [1,2].

In the proton NMR spectrum of complex **1**·HOAc at room temperature there are three singlets of methyl groups of acetato ligands. The significant difference between chemical shifts of bridging OAc ligands in *cis* and *trans* positions to the phosphine bridge ($\delta_{\text{OAc-}trans} - \delta_{\text{OAc-}cis} = 1.15$ ppm) and the small difference between *trans* bridging OAc and axial HOAc ($\delta_{\text{OAc-}trans} - \delta_{\text{HOAc-axial}} = 0.16$ ppm) indicate that the coordination of the *trans* acetato bridge is strongly influenced by the phosphine bridge. There is a broadened signal of methoxy groups of nonmetallated rings at 4.06 ppm. The significant broadening of the signals is also observed in the aromatic range of the spectrum. These results prompted us to investigate the dynamic properties of this compound. The proton spectra and the most likely explanation of them are shown in the Fig. 1 and Scheme 1. Most probably two independent exchange processes are responsible for the dynamic properties of **1**·HOAc. The first one is caused by exchange of methoxy groups of OMP coordinated in axial positions (temperature of coalescence 280 ± 2 K). The second process (temperature of coalescence 259 ± 1 K) is caused by tilting of the phenyl ring forming the –P–C–C–O– bridge with respect to other ligands. There are two possible ways shown of transforming complex **1**·HOAc from the ground state d(S) into the ground state d(R) via an intermediate form (a): d(S)↔c(S)↔a↔c(R)↔d(R) or d(S)↔b↔a↔b↔d(R) (Scheme 1). Comparison of the temperatures of coalescence indicates that the pathway via (c) is a more probable one.

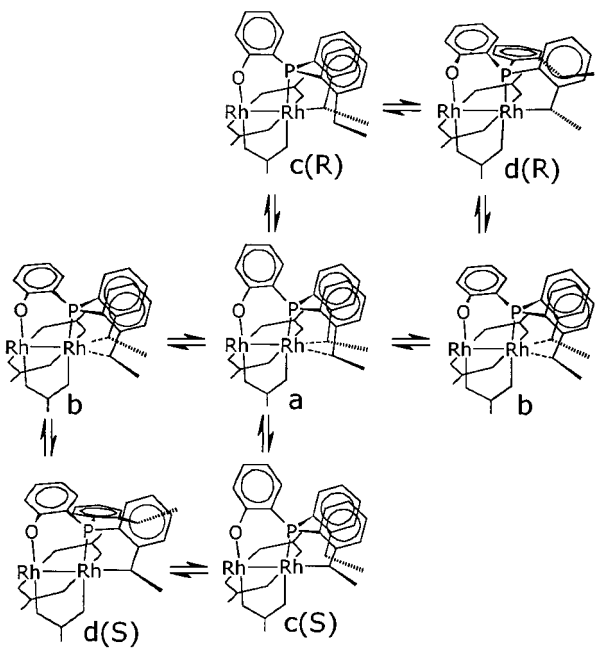

Scheme 1. Representation of possible changes in the structure of compound **1**·HOAc.

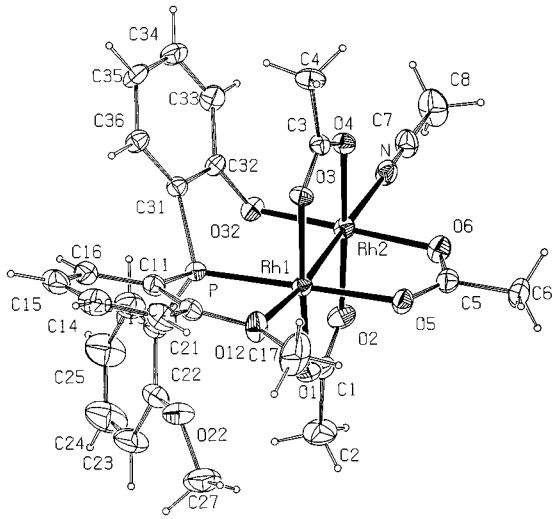

Fig. 2. Crystal structure of **1**·NCMe with the atomic numbering schemes.

2.3. Crystal structure of *1*·NCMe

Compound **1**·NCMe was obtained by the recrystallization of **1**·HOAc in the MeCN–H_2O mixture.

A PLATON-97 [19] drawing of the molecular structures of **1**·NCMe is presented in Fig. 2. Details of crystallographic data collection and structure solution are given in Table 2; fractional coordinates and isotropic thermal parameters are listed in Table 3 and Table 4 contains selected bond lengths and angles for **1**·NCMe. Rhodium atoms in complex **1**·NCMe have distorted octahedral coordination. The dirhodium core is bridged by three acetate groups and one OMP ligand in which the CH_3^+ cation of one of the methoxy substituents is split off and oxygen-metallation has occurred at one of the phenyl rings. The distance Rh(2)–Rh(1) = 2.421(1) Å indicates a rather strong single bond between the two metal atoms, but is distinctly longer than that found in **3**·2(H_2O) (2.3855(5) Å) [20]. Bond lengths between Rh atom and equatorial O atoms are generally the same, as in **3**·2(H_2O) (average 2.0385 Å), except Rh(1)–O(5) (*trans* to Rh(1)–P bond) which is much longer. One axial site of **1** is occupied by a molecule of acetonitrile and another one by a methoxy substituent of one of phenyl rings. The Rh(1)–O(12) distance is considerably longer than the distance Rh–OH_2 (2.310(3) Å) in **3**·2(H_2O).

The molecular structure of **1**·NCMe does not significantly differ from the structure of **1**·HOAc [21]. The small differences in the geometry around the Rh(1)–Rh(2) core are most probably caused by the formation of a strong intermolecular hydrogen bond between O(8) and O(32) atoms in complex **1**·HOAc. This implicates a rather small influence of the axial ligands on the structure of these complexes.

Table 2
Summary of crystal data, data collection and refinement details of complex **1**·NCMe

Crystal data	
Identification code	gp33n
Molecular formula	$C_{28}H_{30}NO_9PRh_2$
Formula weight	761.32
Temperature (K)	293(2)
Radiation type	Mo–K_α
Wavelength (Å)	0.71073
Cell parameters from 5002 reflections	
Crystal system, space group	Triclinic, $P\bar{1}$
Unit cell dimensions	
a (Å)	9.409(2)
b (Å)	9.522(2)
c (Å)	18.234(4)
α (°)	76.28(3)
β (°)	81.82(3)
γ (°)	65.91(3)
Volume (Å^3)	1446.9(5)
Z	2
D_{calc} (Mg m^{-3})	1.747
Absorption coefficient (mm^{-1})	1.250
$F(000)$	764
Crystal size (mm)	$0.2 \times 0.2 \times 0.2$
Data collection	
Radiation source	Fine-focus sealed tube
Radiation monochromator	Graphite
Measurement device type	KM4CCD Kuma Diffraction diffractometer
Measurement method	ω-scans
θ Range for data collection (°)	2.30–29.26
Index ranges	$-12 \le h \le 11$, $-12 \le k \le 12$, $-23 \le l \le 24$
Reflections collected/unique	10 266/5002 [$R_{int} = 0.0217$]
Completeness to $2\theta = 29.26$ (%)	63.7
Absorption correction	Empirical by ψ scan
Refinement	
Refinement method	Full-matrix least-squares on F^2
Data/restraints/parameters	5002/0/368
Goodness-of-fit on F^2	1.190
Final R indices [$I > 2\sigma(I)$]	$R_1 = 0.0308$, $wR_2 = 0.0838$
R indices (all data)	$R_1 = 0.0308$, $wR_2 = 0.0838$
Extinction coefficient	0.0000(2)
Largest difference peak and hole (e Å^{-3})	0.778 and −0.710
Computing data collection	KM4CCD (Kuma Diffraction, 1997) [26]
Computing cell refinement	KM4RED (Kuma Diffraction, 1997) [27]
Computing data reduction	KM4RED (Kuma Diffraction, 1997) [27], XEMP in SHELXTL-PC [28]
Computing structure solution	SHELXS-97 (Sheldrick, 1997) [29]
Computing structure refinement and publication material	SHELXL-97 (Sheldrick, 1997) [30]
Computing molecular graphics	PLATON-97 [19]

Table 3
Atomic coordinates ($\times 10^4$) and equivalent isotropic displacement parameters ($Å^2 \times 10^3$) of the non-H atoms of complex **1**·NCMe

	x	*y*	*z*	U_{eq} [a]
Rh1	9570(1)	6453(1)	2711(1)	21(1)
Rh2	7192(1)	8197(1)	3254(1)	23(1)
P	8530(1)	5157(1)	2263(1)	21(1)
N	5100(5)	9752(4)	3808(2)	31(1)
O1	9188(4)	8194(3)	1767(2)	29(1)
O2	6901(4)	9747(4)	2253(2)	34(1)
O3	9780(3)	4876(3)	3707(2)	24(1)
O4	7604(3)	6541(3)	4221(2)	26(1)
O5	10 748(4)	7532(4)	3149(2)	29(1)
O6	8507(4)	9157(4)	3614(2)	34(1)
O12	11 863(3)	4440(4)	2332(2)	35(1)
O22	10 055(4)	5847(4)	823(2)	41(1)
O32	5837(3)	7350(3)	2881(2)	27(1)
C1	7939(6)	9398(5)	1734(3)	31(1)
C2	7670(7)	10 548(7)	993(3)	51(1)
C3	8732(5)	5240(5)	4227(2)	23(1)
C4	8800(6)	3990(6)	4908(3)	35(1)
C5	9972(6)	8625(5)	3486(2)	30(1)
C6	10 819(6)	9405(6)	3778(3)	39(1)
C7	4043(6)	10 497(6)	4094(3)	34(1)
C8	2674(6)	11 498(7)	4447(4)	54(2)
C11	10 134(5)	3352(5)	2110(2)	24(1)
C12	11 665(5)	3164(5)	2197(2)	26(1)
C13	12 910(6)	1767(6)	2125(3)	39(1)
C14	12 649(7)	570(6)	1953(3)	44(1)
C15	11 177(7)	740(6)	1822(3)	40(1)
C16	9932(6)	2129(5)	1904(3)	32(1)
C17	13 364(4)	4358(7)	2388(2)	70(2)
C21	7611(3)	6037(3)	1371(2)	28(1)
C22	8515(3)	6398(4)	731(2)	35(1)
C23	7806(3)	7215(4)	55(2)	52(2)
C24	6236(8)	7665(9)	14(4)	68(2)
C25	5342(7)	7321(9)	629(4)	64(2)
C26	6035(6)	6503(7)	1305(3)	42(1)
C27	10 940(8)	6595(8)	313(3)	60(2)
C31	7149(5)	4619(5)	2931(2)	23(1)
C32	5972(5)	5900(5)	3202(2)	23(1)
C33	4979(5)	5591(6)	3802(3)	35(1)
C34	5151(6)	4076(6)	4129(3)	38(1)
C35	6302(5)	2827(5)	3854(3)	33(1)
C36	7293(5)	3090(5)	3260(3)	28(1)

[a] U_{eq} is defined as one-third of the trace of the orthogonalized U_{ij} tensor.

2.4. Complexes with DOMP

In $^{31}P\{^1H\}$-NMR spectra of 1:1 and 1:2 mixtures of **3** and DOMP in $CDCl_3$ at room temperature, three signals have been found. The most intense one is a singlet of free phosphine. The less intense are a doublet at 13.2 ppm (^1J(P–Rh) = 162 Hz) and a broad singlet at 11.6 ppm, respectively. The doublet can be assigned to the intermediates in the reaction of the formation of **2**·HOAc, and the broad singlet to $P(2,6\text{-}(OMe)_2C_6H_3)_3Me^+OAc^-$ — the most probable byproduct [2]. Adducts of **3** with the axial DOMP phosphine are not observed, due to the steric hindrances.

$^{31}P\{^1H\}$-NMR of **2**·HOAc shows a doublet centered at 13.6 ppm (^1J(P–Rh) = 151 Hz). The difference between phosphorus chemical shifts in **2**·HOAc and in free ligand ($\Delta\delta(^{31}P) \approx 80$ ppm) is similar to that in **1**·HOAc and in $Rh_2(OAc)_3((2\text{-}OC_6H_2(OMe)_2)P(C_6H_2(OMe)_3)_2)(MeOH)$.

The proton NMR spectrum of compound **2**·HOAc in $CDCl_3$ indicates that all of the methyl groups and phenyl rings are unequivalent because separated signals are observed for each $-CH_3$ group and each aromatic proton. The molecular structure of **2**·HOAc is similar to that of complex **1**·HOAc, as indicated by NMR and UV–vis spectra and analogous mass spectra (see Sections 3.2 and 3.3) The most probable molecular structure of **2**·HOAc is presented in Fig. 3.

2.5. Reactions of *1*·HOAc and *2*·HOAc with carbon monoxide

We have investigated reactions of **3**, **1**·HOAc and **2**·HOAc with CO in $CHCl_3$, MeCN and MeOH. These

Table 4
Selected bond lengths (Å) and angles (°) in complex **1**·NCMe

Bond lengths		*Bond angles*	
Rh(1)–O(3)	2.040(3)	O(3)–Rh(1)–P	87.94(9)
Rh(1)–O(1)	2.043(3)	O(1)–Rh(1)–P	93.88(10)
Rh(1)–O(5)	2.119(3)	O(5)–Rh(1)–P	175.19(9)
Rh(1)–P	2.200(1)	O(3)–Rh(1)–Rh(2)	87.91(9)
Rh(1)–O(12)	2.373(3)	O(1)–Rh(1)–Rh(2)	86.47(10)
Rh(1)–Rh(2)	2.421(1)	O(5)–Rh(1)–Rh(2)	86.79(9)
Rh(2)–O(4)	2.031(3)	P–Rh(1)–Rh(2)	97.49(4)
Rh(2)–O(6)	2.058(3)	O(12)–Rh(1)–Rh(2)	171.28(9)
Rh(2)–O(2)	2.029(3)	O(4)–Rh(2)–O(32)	92.34(12)
Rh(2)–O(32)	2.022(3)	O(2)–Rh(2)–O(32)	87.35(13)
O(32)–C(32)	1.326(5)	O(4)–Rh(2)–Rh(1)	87.44(9)
P–C(31)	1.798(4)	O(6)–Rh(2)–Rh(1)	88.20(9)
P–C(11)	1.816(4)	O(2)–Rh(2)–Rh(1)	88.77(10)
P–C(21)	1.805(3)	O(32)–Rh(2)–Rh(1)	93.42(9)
Rh(2)–N	2.203(4)	C(31)–P–C(11)	107.3(2)
N–C(7)	1.103(6)	C(31)–P–C(21)	107.22(17)
C(7)–C(8)	1.427(7)	C(31)–P–Rh(1)	112.16(14)
		C(32)–O(32)–Rh(2)	117.1(3)
		O(32)–Rh(2)–N	88.95(13)
		N–Rh(2)–Rh(1)	176.66(11)
		N–C(7)–C(8)	178.3(6)

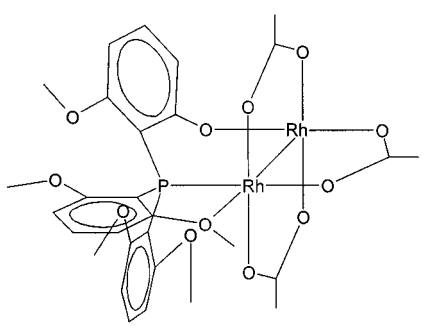

Fig. 3. Proposed molecular structure of **2**.

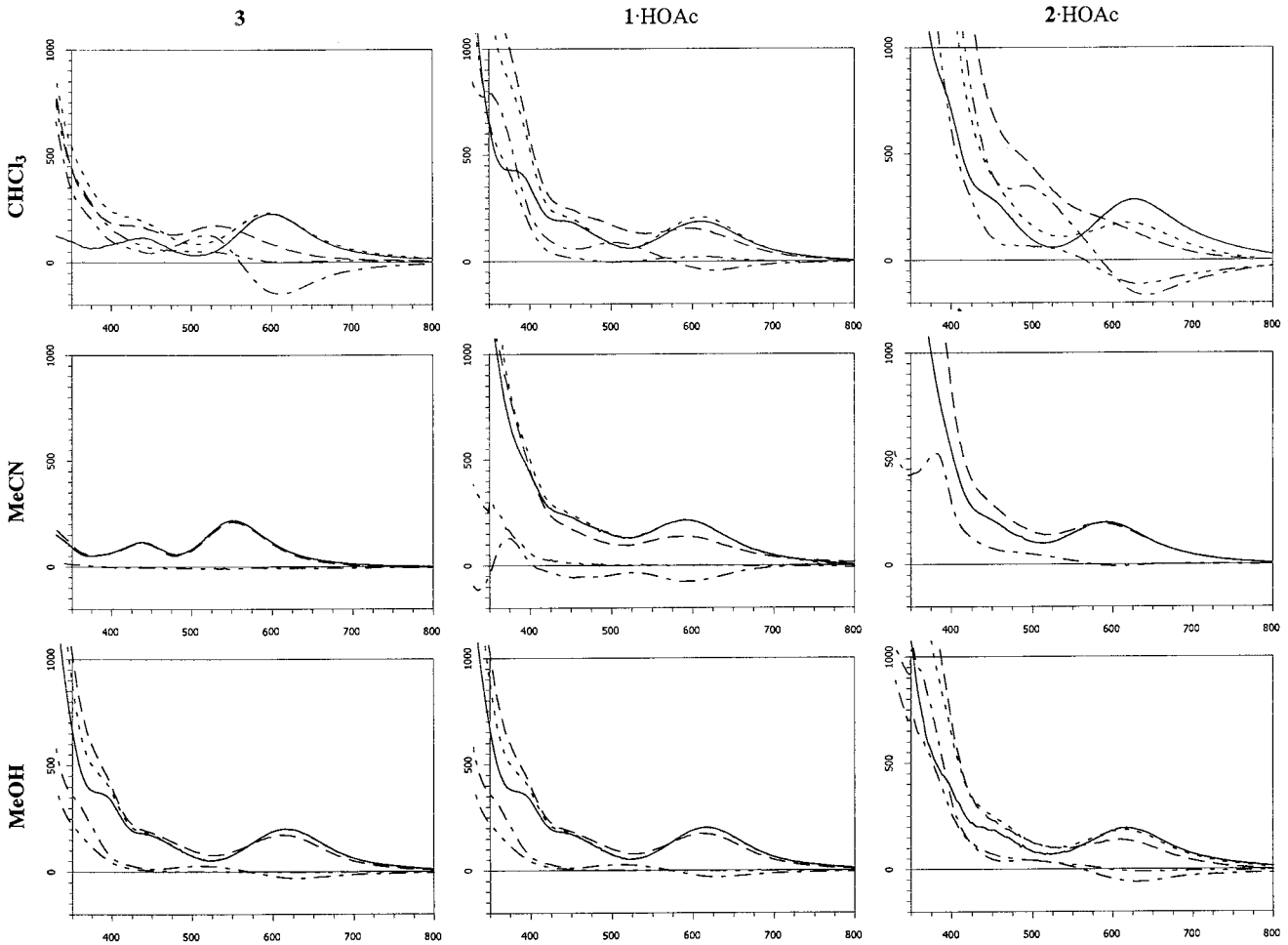

Fig. 4. UV–vis spectra of reactions of **3**, **1**·HOAc and **2**·HOAc in different solvents. Axis of abscissae: λ (nm); axis of ordinates: $Ac_0^{-1}\,l^{-1}$ ($dm^3\,mol^{-1}\,cm^{-1}$). Lines: (––––) parent complex, (– – – –) complex in CO atmosphere, (–.–.–.) difference spectrum of the complex in CO atmosphere against the parent complex, (.....) complex after reaction with CO in N_2 atmosphere, (–..–..–) difference spectrum of the complex in N_2 atmosphere against the parent complex.

reactions were monitored by UV–vis spectroscopy. The coordination of CO ligands in axial positions causes considerable blue shift of the first band assigned to the $\pi^*(Rh_2) \rightarrow \sigma^*(Rh_2)$ transition, in the case of all complexes (Fig. 4). These shifts are expected for the CO adducts because the CO ligand has a very large 10Dq value and also shows strong acceptor properties [18,22].

In the case of complex **3** in $CHCl_3$ the first band is shifted from 599 to 530 nm for CO adducts. The blue shift for complex **2** and its adduct **2**·2CO in $CHCl_3$ is similar (from 626 to 590 nm). The blue shift for CO adducts of complex **1** in $CHCl_3$ is very small. This suggests mainly formation of monoadduct **1**·CO. This conclusion was confirmed by IR and NMR spectroscopy. In MeCN and MeOH blue shifts of all complexes are very small. The reactivity of the investigated complexes towards CO depends on the reacting complex and solvent used; **3** forms adducts with CO only in $CHCl_3$; MeCN and MeOH seem to coordinate more strongly than carbon monoxide. Compound **2**·HOAc forms an adduct with CO in $CHCl_3$; in MeCN and MeOH only weak interactions can be observed. Compound **1**·HOAc weakly interacts with CO in all these solvents. In all cases, changing the atmosphere to N_2 leads to the removal of the CO ligand from the coordination sphere, which indicates that adducts $[Rh_2(bridge)_4L(CO)]$ are labile and the Rh–CO bond is weak. The reaction was reversible through many numbers of cycles by alternately changing CO and N_2 atmosphere. Reactions of **1**·HOAc and **2**·HOAc with CO in $CHCl_3$ were also investigated in the temperature range 298–333 K. The increase of temperature to 333 K leads to UV–vis spectra that are very similar to the spectra obtained at 298 K under N_2. This is most likely caused by the low stability of complexes containing carbonyl ligands and to some extent by the lower solubility of CO at higher temperatures.

Some of the products and intermediates were analyzed also by IR and NMR spectroscopy.

The ^{1}H-NMR spectrum of **2**·*n*CO in $CDCl_3$ saturated with CO at room temperature does not differ much from the spectrum of **2**·HOAc. We have observed only small changes of chemical shifts and coupling constants. The $^{31}P\{^1H\}$-NMR spectrum is much more different from the analogous spectrum of **2**·HOAc; at this temperature it shows only a broad doublet at 8.85 ppm (^1J(P–Rh) = 161 Hz). The intensity increases with decreasing the temperature to 243 K.

The $^{13}C\{^1H\}$-NMR spectrum of the adduct of **2** with ^{13}CO at room temperature shows only a broad singlet of CO at 158 ppm. Its intensity is much higher than for other ligands with natural abundance of ^{13}C. The presence of a broad signal is indicative of exchange processes between CO bonded to the complex and free CO. At 243 K CO shows a doublet of doublets at 153 ppm (^1J(C–Rh) = 42.0 and ^2J(C–Rh) = 12.7 Hz). These data indicate formation of the monoadduct of **2**·CO, in which the CO replaces axial HOAc ligand. The chemical shift $\delta(^{13}C)$ and ^1J(C–Rh) for this adduct are much lower than those for the complex $Rh_2(OAc)_2(C(O)OMe)_2(CO)_2(MeOH)_2$ containing CO ligands in equatorial coordination sites ($\delta C(^{13}CO)$ = 186.6 ppm and ^1J(C–Rh) = 74.6 Hz) [23]; however, chemical shifts of CO ligands in carbonyl complexes in higher oxidation states are lower in comparison with other carbonyl complexes [24]. NMR spectra of **1**·*n*CO in the same conditions generally differ from the spectra of **1**·HOAc. The $^{31}P\{^1H\}$-NMR spectrum shows a weak and broad doublet at 32.9 ppm (^1J(P–Rh) = 154 Hz), in ^{1}H-NMR spectrum all signals are significantly broadened. The $^{13}C\{^1H\}$-NMR spectrum of complex **1**·*x*CO in ^{13}CO atmosphere at 243 K shows two signals of CO ligands: a doublet of doublets at 144 ppm (^1J(C–Rh) = 42.0 and ^2J(C–Rh) = 6.3 Hz) and a weaker, broad doublet at 142 ppm (^1J(C–Rh) = 42 Hz). These signals correspond to two sets of signals in the ^{1}H-NMR spectrum. In ^{1}H-NMR spectrum of **1**·*n*CO signals of methoxy groups of higher intensity (amount 68%) are at 4.76 and 3.40 ppm and signals of methoxy groups of lower intensity (amount 32%) are at 3.65 and 3.13 ppm, with differences in chemical shifts of the signals in the sets 1.36 and 0.52 ppm, respectively. This suggests a formation of the monoadduct **1**·CO and bisadduct **1**·2CO in which CO most probably replaces the coordinated –OMe group of phosphine ligand. This conclusion was also confirmed by IR spectra of the complexes in $CHCl_3$ solutions in which two bands assigned to the stretching CO vibrations were observed at 2085 and 2105 cm^{-1}. The ratio of intensity of these signals is ca. 2:1 and is similar to that observed in the ^{1}H-NMR spectrum. In the IR spectrum of adduct **2**·CO only one band in the CO region was observed at 2084 cm^{-1}, which also confirms the NMR data indicating that this complex forms only a monoadduct. In analogous conditions complex **3** forms bisadduct **3**·2CO, because in the IR spectrum only one band at 2105 cm^{-1} was found; the same frequency was observed for solid **3**·2CO [6].

The possibility of the substitution of the methoxy group from the axial coordination site in **1**·HOAc core by other ligands was investigated by measuring spectra of **1** in CD_3CN and in $CDCl_3$ with a small amount of CH_3CN at low temperatures. At 283 K in CD_3CN the results were very similar to those obtained for **1**·*x*CO in $CDCl_3$. The higher signals of methoxy group are at 4.58 and 3.42 ppm (the difference between their positions is 1.16 ppm) and the lower ones are at 3.57 and 3.04 ppm (difference: 0.53 ppm). In the $CDCl_3$–CH_3CN mixture the results are as follows: 4.73 and 3.38 ppm (amount 92%; difference 1.35 ppm) for the set of signals of high intensity and for signals of very low intensity 3.59 and 3.10 (amount 8%; difference 0.49 ppm). Obtained results indicate that substitution of axial methoxy ligand by another more strongly coordinating one takes place and depends on the concentration of substituting ligand. These data indicate that for monoadducts **1**·CO and **1**·MeCN the difference between the chemical shifts of the methoxy groups is much higher (ca 1.35 ppm) than that for bisadducts **1**·2CO and **1**·2MeCN, 0.52 ppm and 0.49 ppm, respectively. The large difference between chemical shifts of methoxy groups in monoadducts proves that one axial coordinating site is occupied by CO or MeCN ligand and the other by a methoxy group. Thus methoxy groups are relatively strongly coordinated with rhodium and in solutions in noncoordinating solvents, one methoxy group is bound with rhodium in axial position.

3. Experimental

3.1. Procedures and materials

Complex $[Rh_2(OAc)_4]$ (**3**) [25] was prepared by the literature method. Phosphine ligands OMP and DOMP were obtained from Strem and Avocado, respectively and used without further purification. All solvents were deoxidized prior to use.

All operations were performed in a dinitrogen atmosphere using standard Schlenk techniques. Infrared spectra (KBr pellets) were measured on a Bruker IFS 113v and UV–vis spectra on a Beckman DU 7500 spectrometer. ^{1}H-NMR and $^{31}P\{^1H\}$-NMR spectra were measured on a Bruker AMX 300 spectrometer using 85% H_3PO_4 in H_2O as an external standard for ^{31}P. Mass spectra were measured on a Finnigan Mat TSQ 700 ESI in $CHCl_3$.

3.2. Synthesis of $[Rh_2(OAc)_3\{\mu\text{-}(C_6H_4\text{-}2\text{-}O)P(C_6H_4\text{-}2\text{-}OMe)_2\}](HOAc)$ (**1**·HOAc)

A mixture of $[Rh_2(OAc)_4]$ (0.177 g, 0.4 mmol) and OMP (0.282 g, 0.8 mmol) in 10 cm^3 of ethanol and 10 cm^3 of acetic acid was refluxed with stirring for 7 h. A crystalline product was obtained after slow evaporation of the solvents (to 0.5 of initial volume). Yield 0.203 g, 65%. Anal. Calc. for $C_{28}H_{31}O_{11}PRh_2$: C, 43.10; H, 4.00; P, 3.97. Found: C, 43.0; H, 3.9; P, 3.9%. MS: 661.3 $\{Rh_2(OAc)_2(OC_6H_4)P(C_6H_4OMe)_2\}^+$, 721.4 $\{Rh_2(OAc)_3(OC_6H_4)P(C_6H_4OMe)_2\cdot H\}^+$, 742.8 $\{Rh_2(OAc)_3(OC_6H_4)P(C_6H_4OMe)_2\cdot Na\}^+$, 852.6, 1321.5, 1381.9 $\{[Rh_2(OAc)_3(OC_6H_4)P(C_6H_4OMe)_2]_2 + \{[Rh_2(OAc)_2(OC_6H_4)P(C_6H_4OMe)_2]_2\}^+$, 1440.9 $\{[Rh_2(OAc)_3(OC_6H_4)P(C_6H_4OMe)_2]_2\}^+$, 1463.1 $\{[Rh_2(OAc)_3(OC_6H_4)P(C_6H_4OMe)_2]_2\cdot Na\}^+$, 1478.6, 1524.7.

3.3. Synthesis of $[Rh_2(OAc)_3\{(C_6H_3\text{-}6\text{-}OMe\text{-}2\text{-}O)P(C_6H_3\text{-}2,6\text{-}(OMe)_2)_2\}](HOAc)$ (**2**·HOAc)

A mixture of $[Rh_2(OAc)_4]$ (0.221 g, 0.5 mmol) and OMP (0.442 g, 1.0 mmol) in 15 cm^3 of ethanol was refluxed with stirring for 8 h. After addition of ca. 3 cm^3 of water, the precipitated product was filtered and washed with water. Yield 0.226 g, 52%. Anal. Calc. for $C_{31}H_{37}O_{14}PRh_2$: C, 42.78; H, 4.28; P, 3.56. Found: C, 42.7; H, 4.2; P, 3.5%. MS: 457.6, 612.2, 751.8 $\{Rh_2(OAc)_2(OC_6H_3OMe)P(C_6H_3(OMe)_2)_2\}^+$, 811.3 $\{Rh_2(OAc)_3(OC_6H_3OMe)P(C_6H_3(OMe)_2)_2\cdot H\}^+$, 837.4, 957.6, 1561.1 $\{[Rh_2(OAc)_3(OC_6H_3OMe)P(C_6H_3(OMe)_2)_2]_2 + \{[Rh_2(OAc)_2(OC_6H_3OMe)P(C_6H_3(OMe)_2)_2]_2\}^+$, 1620.3 $\{[Rh_2(OAc)_3(OC_6H_3OMe)P(C_6H_3(OMe)_2)]_2\}^+$, 1643.3 $\{[Rh_2(OAc)_3(OC_6H_3OMe)P(C_6H_3(OMe)_2)]_2\cdot Na\}^+$, 1767.9.

3.4. Reactions with CO

Samples of **1**·HOAc or **2**·HOAc were dissolved and bubbled with pure CO from 0.5 to 2.0 h. Due to instability of products, UV–vis and NMR spectra were prepared in situ.

3.5. X-ray crystallographic measurements

X-ray data were collected and processed with Mo–K_α radiation at 293 K on a Kuma Diffraction KM4CCD diffractometer using the original KM4CCD data collection program [26] and KM4RED data reduction program [27]. The intensities were corrected for the Lorentz and polarization effects and for empirical absorption [28]. The structure was solved by direct methods using the SHELXS program [29] and refined on F^2 values by full-matrix least-squares using the SHELXL program [30] from the SHELX-97 system, with anisotropic temperature factors for non-hydrogen atoms. Positions of hydrogen atoms are found from ΔF syntheses or geometrically and refined in rigid groups with the heavy atoms connected to them. A summary of crystal data and details of data collection and structure refinement are given in Table 1.

4. Supplementary material

Structure factors can be obtained from the author (E.G.). Anisotropic displacement parameters and hydrogen atom parameters have also been deposited with the Cambridge Crystallographic Data Centre, 12 Union Road, Cambridge CB2 1EZ, UK.

Acknowledgements

The financial support of this research by KBN (Grant 3-T09A-023-14) is greatly appreciated.

References

[1] S.J. Chen, K.R. Dunbar, Inorg. Chem. 29 (1990) 590.
[2] S.J. Chen, K.R. Dunbar, Inorg. Chem. 30 (1991) 2018.
[3] K.R. Dunbar, J.H. Matonic, V.P. Saharan, Inorg. Chem. 33 (1994) 25.
[4] C.J. Alarcon, P. Lahuerta, E. Peris, M.A. Ubeda, A. Aguuirre, S. Garcia-Granda, F. Gomez-Beltran, Inorg. Chim. Acta 254 (1997) 177.
[5] F.P. Pruchnik, R. Starosta, T. Lis, P. Lahuerta, J. Organomet. Chem. 568 (1998) 177.
[6] G.G. Christoph, Y.-B. Koh, J. Am. Chem. Soc. 101 (1979) 1422.
[7] R.S. Drago, S.P. Tanner, R.M. Richman, J.R. Long, J. Am. Chem. Soc. 101 (1979) 2898.
[8] R.B. King, A.D. King Jr., M.Z. Iqbal, J. Am. Chem. Soc. 101 (1979) 4893.
[9] C. Bilgrien, R.S. Drago, G.C. Vogel, J. Stahlbush, Inorg. Chem. 25 (1986) 2864.
[10] J.L. Bear, C.-L. Yao, L.-M. Liu, F.J. Capdevielle, J.D. Korp, T.A. Albright, S.-K. Kang, K.M. Kadish, Inorg. Chem. 28 (1989) 1254.
[11] P. Lahuerta, J. Paya, X. Solans, M.A. Ubeda, Inorg. Chem. 31 (1992) 385.
[12] P. Lahuerta, J. Paya, E. Peris, A. Aguirre, S. Garcia-Granda, F. Gomez-Beltran, Inorg. Chim. Acta 192 (1992) 43.
[13] P. Lahuerta, J. Paya, M.A. Pellinghelli, A. Tripicchio, Inorg. Chem. 31 (1992) 1224.
[14] F. Estevan, S. Garcia-Granda, P. Lahuerta, J. Latorre, E. Peris, M. Sanau, Inorg. Chim. Acta 229 (1995) 365.
[15] E.B. Boyar, S.D. Robinson, Inorg. Chim. Acta 64 (1982) L193.
[16] E.B. Boyar, S.D. Robinson, Inorg. Chim. Acta 76 (1983) L137.
[17] E.B. Boyar, S.D. Robinson, J. Chem. Soc. Dalton Trans. (1985) 629
[18] F.P. Pruchnik, R. Starosta, P. Smoleński, E. Shestakova, P. Lahuerta, Organometallics 17 (1998) 3684.
[19] A.L. Spek, PLATON-97, Bijvoet Centre for Biomolecular Research Vakgroep Kristal and Structuurchemie, Utrecht University, The Netherlands.
[20] F.A. Cotton, B.G. DeBoer, M.D. LaPrade, J.R. Pipal, D.A. Ucko, Acta Crystallogr. Sect. B 27 (1971) 1664.

[21] Z. Gałdecki, E. Gałdecka, A. Kowalski, F.P. Pruchnik, K. Wajda-Hermanowicz, R. Starosta, Polish J. Chem. 73 (1999) 859.
[22] L. Natkaniec, F.P. Pruchnik, J. Chem. Soc. Dalton Trans. (1994) 3261
[23] Y.S. Varshavsky, T. Cherkasova, Rhodium Express 15 (1996) 13.
[24] J. Browning, P.L. Goggin, R.J. Goodfellow, M.G. Norton, A.J.M. Rattray, J. Chem. Soc. Dalton Trans. (1977) 2061
[25] G.L. Rempel, P. Legzdins, H. Smith, G. Wilkinson, Inorg. Synth. 13 (1974) 90.
[26] KM4CCD, Data Collection Program, Kuma Diffraction Ltd., Wrocław, Poland, 1997.
[27] KM4RED, Data Reductions Program, Kuma Diffraction Ltd., Wrocław, Poland, 1997.
[28] G.M. Sheldrick, SHELXTL-PC, Version 4.2, Siemens Analytical X-ray Instruments Inc., Madison, WI, 1991.
[29] G.M. Sheldrick, SHELXS-97, Program for the Solution of Crystal Structures, University of Göttingen, Germany, 1997.
[30] G.M. Sheldrick, SHELXL-97, Program for the Refinement of Crystal Structures, University of Göttingen, Germany, 1997.